Chinese Chemical Letters 36 (2025) 110297

Contents lists available at ScienceDirect

Chinese Chemical Letters

journal homepage: www.elsevier.com/locate/cclet

On-target site enriching fluorescent bioprobe for imaging of receptor tyrosine kinase in tumor

Meng Gao[a], Jiqiu Yin[b], XianChao Jia[a], Ye Gao[a], Yang Jiao[a,*]

[a] School of Chemistry, Dalian University of Technology Dalian 116024, China
[b] College of Medical Laboratory, Dalian Medical University, Dalian 116044, China

ARTICLE INFO

Article history:
Received 3 June 2024
Revised 24 July 2024
Accepted 26 July 2024
Available online 26 July 2024

Keywords:
Receptor tyrosine kinases
Fluorescent bioprobe
Host-guest system
On-target site enriching
Tumor diagnosis

ABSTRACT

Receptor tyrosine kinases (RTKs) are biological enzymes expressed on cell membranes that can influence cellular signaling, and their overexpression in tumor cells makes them a key route to assess relevant tumor processes. The development of a delivery system that targets and accumulates in RTKs overexpressing-cells at the on-target site is significant for the monitoring of tumor progression and clinical applications through longer tumor site signaling response under low injection frequency. Here, a host-guest nanoscale fluorescent probe SNI@ZIF-8 based on zeolitic imidazolate framework-8 (ZIF-8) and a fluorescent probe SNI constructed from receptor tyrosine kinase inhibitor was proposed and prepared for targeting RTKs and enabling prolonged fluorescence imaging *in vivo*. The folded conformation of the probe SNI resulted in low background fluorescence, and the unfolding of the SNI conformation upon insertion of the RTKs active pocket showed significant fluorescence enhancement thus enabling real-time detection of RTKs. The host-guest system SNI@ZIF-8 could release guest molecules due to the presence of the enzyme, emphasizing the reporting of stable fluorescent signals over time under low injection frequency. SNI@ZIF-8 could provide a signal response on the cell membrane of RTKs overexpressing cells without interference from other substances, and provided a longer fluorescent signal than SNI at equivalent number of injections in tumor-bearing mice. The host-guest system SNI@ZIF-8, with its obvious tumor site enrichment ability and clear fluorescence imaging ability, could be successfully applied to the detection of RTKs on cell membranes in biological systems, providing a new strategy for determining the process of tumor development in clinical applications.

Receptor tyrosine kinases (RTKs) are the natural and essential messenger of cancer cells to promote communication between cells and participate in many biological regulatory processes, associating with cell growth, motility, differentiation and metabolism, and their overexpression usually occurs to a sequence of events, including cancer cells metastasis and local angiogenesis during tumor progression [1-4]. Molecule fluorescence probes provide a potential modality for differentiating tumor tissues and guiding clinical procedures, which could show a signal response to report relevant cancers focus on RTKs overexpressing, due to their non-invasive nature, structural adaptability, low cost, and real-time monitoring capabilities [5-7]. Despite fluorescent imaging probes exhibit characteristics such as excellent selectivity and distinct optical signals, the maximizing delivery to the on-target site and reducing non-essential exposures to off-target site to reduce total drug injection remains a much-needed core requirement to RTKs imaging in clinical application [8-11]. Consequently, developing a controllable and homogeneous delivery system, which could enable on-target site enrichment to achieve accumulation in RTKs overexpressing cells and is capable of bioimaging for as long as possible under low injection frequency, is still of significant importance [12,13].

A controllable and homogeneous host-guest system could be preparation by means of non-covalent interactions, helping encapsulate the guest fluorescent probe in the enriched pore channel of the host, to achieve functional integration of good optical signaling and on-target site enrichment in tumors [14-16]. Linear molecular probes are designed to target RTKs that are highly enriched in tumor cell membranes, and are suitable for lining up on the membrane surface to report better signal response. Metal-organic framework (MOF) could be controlled by ligands and metal nodes to modulate their pore channels, making the extent of MOF easier to match linear molecular probes without affecting the nature idiosyncrasy of the molecule itself. The MOF-based host-guest

* Corresponding author.
E-mail address: jiaoyang@dlut.edu.cn (Y. Jiao).

https://doi.org/10.1016/j.cclet.2024.110297
1001-8417/

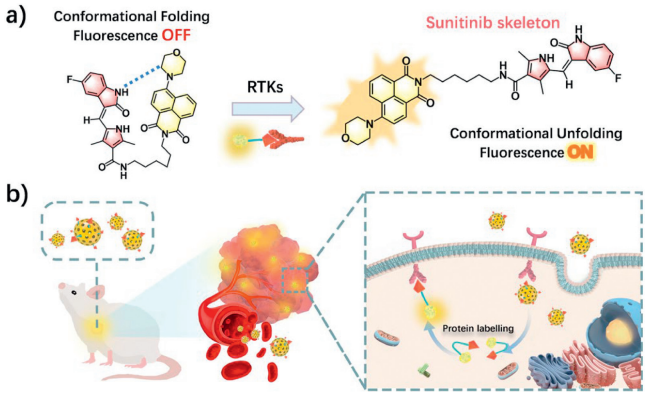

Scheme 1. (a) Fluorescence recovery mechanism of probe SNI. (b) SNI@ZIF-8 cell imaging diagram of targeting tumors.

system could have stable amphiphilicity and non-covalent bond-driven dynamic properties to facilitate functional integration, and the enhanced permeability and retention (EPR) effect of the nanoparticle-sized MOF could pool the fluorescent properties of the guest molecules and the targeting enrichment ability of the host at the tumor site [18,19]. Notably, the role of metal ions in immunotherapy has been extensively investigated in recent years, and the use of MOF themselves or the composition of metal ions released from them to modulate the immune response could provide unexpected functional additions to the host-guest system [20-23]. Using MOF and fluorescent probe to construct a host-guest system, targeting RTKs overexpressed in cancer cells, could help to achieve on-target site accumulation, improve signaling efficiency, and achieve prolonged bio-imaging under low injection frequency [24].

Herein, zeolitic imidazolate framework-8 (ZIF-8) and a fluorescent probe SNI, consisting of sunitinib (RTKs inhibitor) and a naphthalimide derivative, were chosen to form a host-guest system SNI@ZIF-8 through non-covalent interactions, which is capable of enrichment in tumor site and rapidly responding to RTKs in biological systems (Scheme 1). The guest probe SNI exhibited good signal response to RTKs in simulated physiological media, with fluorescence emission intensity about 1.7 fold of the initial fluorescence in 5 min, showing high sensitivity, selectivity and photostability. The host ZIF-8 with abundant porosity and high biocompatibility is favorable for the encapsulation of linear molecules and biological applications, and the lower background fluorescence is more conducive to the signal monitoring of the guest molecule. SNI@ZIF-8 exhibited fluorescent signals to RTKs in solvent and was able to image tumor sites for more than 12 h in tumor-bearing mice. The RTKs inhibitor skeleton in SNI and the targeted aggregation of SNI@ZIF-8 lead to elevated Zn^{2+} concentrations in tumor cells, both of which affect intracellular protein expression and intracellular signaling, with having potential for immunotherapy in clinic. Possessing the advantages of targeting enrichment ability well-defined fluorescent signal and high biocompatibility, the host-guest system SNI@ZIF-8 enabled fluorescent tracking of RTKs on cell membranes, realizing long-time imaging of tumor regions at low injection frequency.

SNI was prepared by a simple three-step organic synthesis, in which the sunitinib is a tyrosine kinase inhibitor that targets vascular endothelial growth factor receptor 2 (VEGFR-2) approved by Food and Drug Administration (FDA), and its molecular skeleton as the recognition group is expected to target receptor tyrosine kinases [25,26]. Naphthalimide was chosen to be the fluorophore, and the hydrophilic morpholine group was introduced into the naphthalene ring of naphthalimide to improve the probe water solubility. The structure of SNI was well characterized by ^{1}H nuclear magnetic resonance (^{1}H NMR), electronspray ionization mass spectrometry (ESI-MS) and 2D NMR analyses (Figs. S1–S6 in Supporting information). Simultaneously, relatively long flexible chain 1,6-hexylenediamime helps it fold, and thus reduces the background fluorescence [27] as shown in cross signal between H_a of the sunitinib group and H_b of the naphthalimide derivant (Fig. 1b). The good photostability of fluorescent probe is particularly important for application in the actual environment. SNI has relatively stable fluorescence properties in solvents, fluorescence enhanced transformation of SNI was directly observed and the fluorescence intensity titration curve would reach a plateau for at least 5 min after adding VEGFR-2 [28] from 0 to 0.27 μg/mL (Fig. 1c). Molecular docking method was used to determine the conformation of SNI and VEGFR-2, CYS-919 and ASP-1052 could form hydrogen bonds

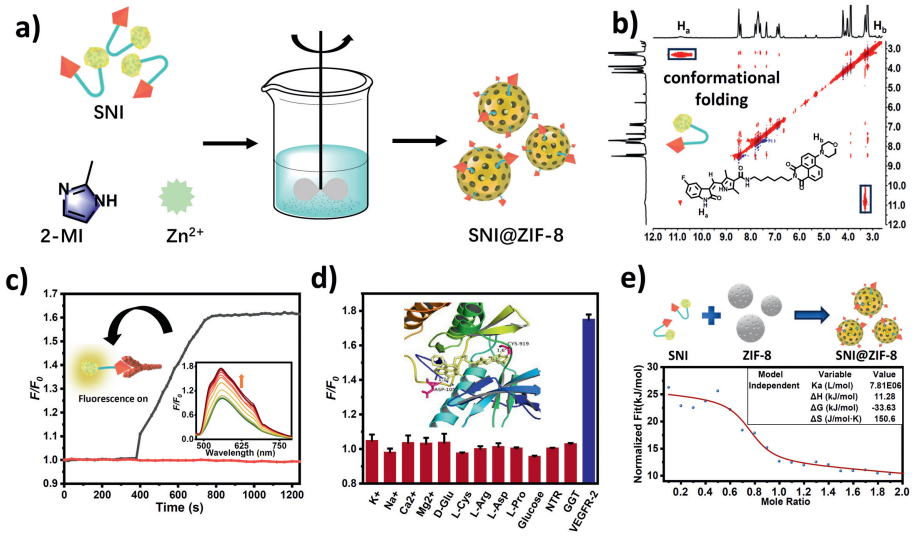

Fig. 1. (a) Assembly diagram of SNI@ZIF-8. (b) Recognition mechanism of small molecule fluorescent probe. (c) Fluorescence responses of SNI (4 μmol/L) to various concentrations of tyrosine kinase DMSO/HEPES (5.5:4.5, v/v, pH 7.4). Time-dependent probe SNI (4 μmol/L) (red line) and fluorescence response of probe with the addition of VEGFR-2 (black line). F_0 is the peak fluorescence intensity of the probe in solvent condition. (d) Fluorescence responses of probe SNI to various interferences and the data were acquired in DMSO/HEPES (5.5:4.5, v/v, pH 7.4) solution. Data are presented as mean ± standard deviation (SD) ($n = 3$). Stereo views of SNI with VEGFR-2 (PDB: 4AGD). (e) The ITC experiments were performed by an isothermal titration microcalorimeter at atmospheric pressure, giving the K_a and the thermodynamic parameters.

with SNI, and the interaction between these groups is the key factor for SNI to recognize VEGFR-2 [29]. SNI has a distinct selectivity for VEGFR-2 compared to other substances present in cells, including K^+, Na^+, Ca^{2+}, Mg^{2+}, D-Glu, L-Cys, L-Arg, L-Asp, L-Pro, nitroreductase (NTR), γ-glutamyltranspeptidase (GGT) and glucose, demonstrating the potential of probe SNI for fluorescence recognition in complex cellular environments (Fig. 1d). Sunitinib can specifically target tyrosine kinase activity domain and, VEGFR-2 kinase activity assays was measured by quantitating the amount of ATP correlated with the amount of kinase activity (Table S1 in Supporting information). The half maximal inhibitory concentration (IC_{50}) value was 1.5 ± 0.1 μmol/L (Fig. S19 in Supporting information). The probe SNI maintained an active state as receptor tyrosine kinase inhibitor in complex media, and it can effectively target the VEGFR domain pocket to inactive enzyme and hinder downstream phosphorylation process. SNI has binding with receptor tyrosine kinases as targeting groups at the micromolar concentrations. The binding affinity of the probe SNI specifically make it targeting receptor tyrosine kinases. To summarize, the experimental results described above show that probe SNI is very suitable for imaging RTKs under solvent conditions, which provided basic support for subsequent experiments. In particular, isothermal titration calorimetry (ITC) with a strong binding effect between SNI and ZIF-8, the association constants (K_a) is 7.81×10^6 L/mol, which provided experimental support for further encapsulation [30], verified that SNI is the ideal element for constructing host-guest nanoscale fluorescent probe for its exceptional host-guest matching (Fig. 1e).

Constructing host-guest system through SNI could achieve delivery and stable imaging due to the good recognition targeting and signaling response to RTKs. SNI@ZIF-8 was synthesized by one-pot method (Fig. 1a) [31]. Probe SNI, zinc ion and 2-methylimidazole were stirred at room temperature in a mixture of water and DMSO, and the supernatant was obtained after centrifugation. The carrying capacity of the probe SNI was calculated as 0.8 wt% by ultraviolet spectroscopy of supernatant (Figs. S11 and S12 in Supporting information). The particle size before and after loading was 265.3 and 329.5 nm, respectively, and the structure of the particle did not change significantly shown as X-ray diffraction (XRD) (Fig. 2a and Fig. S9 in Supporting information) [32]. N_2 adsorption-desorption experiment (Fig. 2b) further confirmed the successful loading of SNI [33]. The decrease of pore capacity indicates that SNI enter the pore of ZIF-8 and the loading behavior has little effect on the pore size of ZIF-8. Compared with unloaded ZIF-8, the characteristic peaks of SNI were shown in the infrared spectra, solid ultraviolet spectra and X-ray photoelectron spectroscopy (XPS) spectra of SNI@ZIF-8 (Figs. 2c and d, Fig. S15 in Supporting information), which further proved the successful loading of SNI [34]. It is demonstrated that SNI@ZIF-8 had good stability, enabling to be further applied. The release of SNI triggered by the enzyme was detected by incubating RTKs with SNI@ZIF-8 (Fig. 2e). Shaking the dialysis bag of SNI@ZIF-8, samples were taken at intervals to detect the fluorescence intensity of the solution, which could help to compare whether the presence of RTKs triggers the release of guest molecules within the host-guest system. The experimental results showed that the addition of RTKs in the host-guest system can trigger the release of SNI and lead to increased fluorescence intensity. The fluorescence signal providing capability of SNI@ZIF-8 was evaluated by adding RTKs to SNI@ZIF-8 and observing the fluorescence changes in the mixed system (Fig. 2e). The results showed that the fluorescence intensity appeared immediately after the addition of VEGFR-2 in SNI@ZIF-8, indicating that the addition of SNI in ZIF-8 could provide certain targeting effect for nanoparticles. With the extension of incubation time, the fluorescence intensity of the system also gradually increased, indicating that VEGFR-2 gradually adsorbed the SNI in the ZIF-8 channel and realized the detection in a long time. In Fig. 2f, the shape of peaks attributable to VEGFR-2 had little change, and the circular dichroism (CD) value had increased before and after adding SNI, suggesting the secondary and tertiary structures of VEGFR-2 preserved and the intermolecular interaction between receptor tyrosine kinase and SNI [35]. It is certificated that the interaction between VEGFR-2 and SNI is conducive to the removal of SNI from the spatial structure of ZIF-8 and the specific recognition between SNI and receptor tyrosine kinase VEGFR-2.

The results of cytotoxicity tests showed that SNI@ZIF-8 had high biocompatibility, indicating its potential biological application

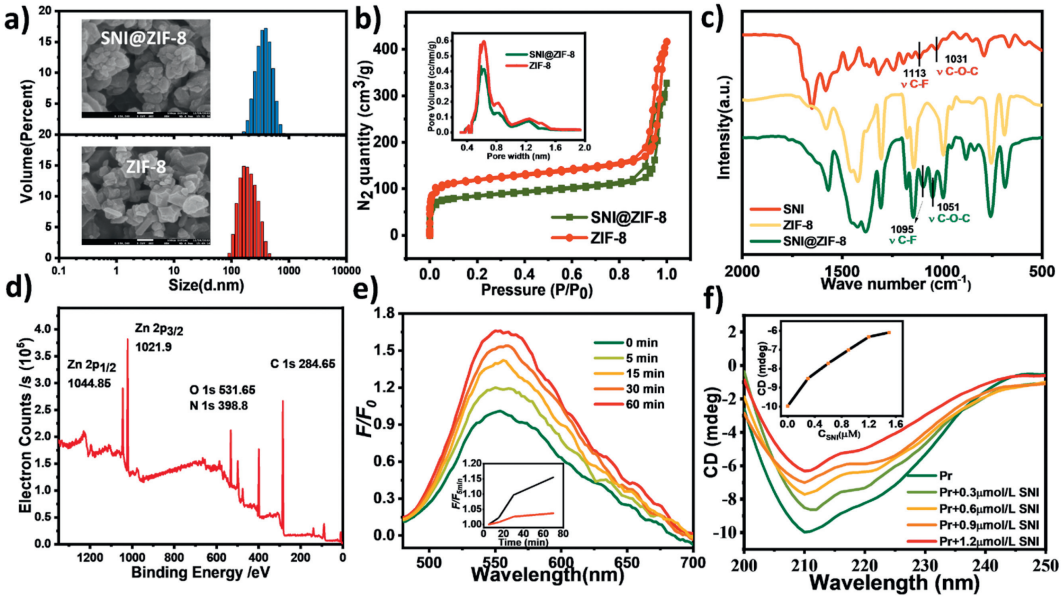

Fig. 2. (a) Dynamic laser light scattering of SNI@ZIF-8 (blue) and ZIF-8 (red) with their scanning electron microscope pictures. Scale bar: 100 nm. (b) N_2 quantity and pore volume of ZIF-8 or SNI@ZIF-8. (c) Infrared spectroscopy (IR) spectra of SNI (orange), ZIF-8 (blue), and SNI@ZIF-8 (mazarine). (d) XPS spectra of SNI@ZIF-8, 531.65 eV is O peak of SNI@ZIF-8. (e) The fluorescence intensity of SNI@ZIF-8 incubated with VEGFR-2 in DMSO/HEPES (5.5:4.5, v/v, pH 7.4) solution changed with time (0–70 min), inset shows fluorescence intensity *versus* the concentrations of SNI. Inset shows the release of SNI in the presence (black) or absence (red) of the enzyme. (f) CD spectra of VEGFR-2 (200 μg/mL) with the increasing addition of SNI from 0 to 1.2 μmol/L. Inset shows CD values at 210 nm *versus* the concentrations of SNI.

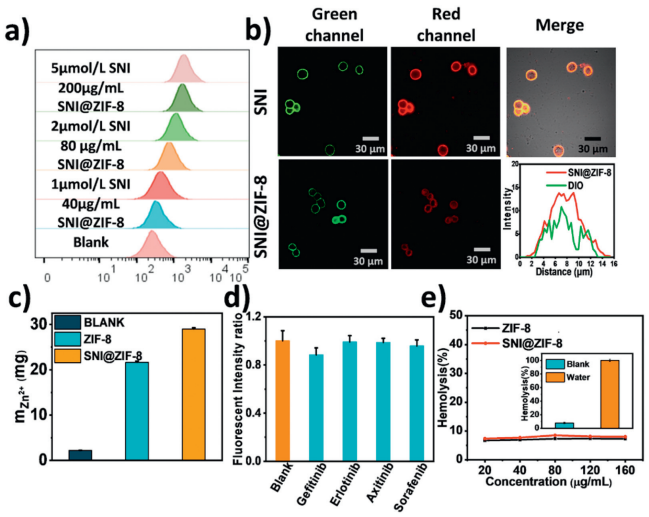

Fig. 3. (a) Flow cytometry treated with different concentrations of SNI and SNI@ZIF-8. (b) Imaging of HT-29 cells treated with 2 μmol/L SNI or 60 μg/mL SNI@ZIF-8. (c) Cell uptake assay by ICP-MS. (d) Relative fluorescence intensity for the HT-29 cells after treatment with gefitinib, erlotinib, axitinib and sorafenib. (e) Hemolysis tests of ZIF-8 and SNI@ZIF-8. Data are presented as mean ± SD ($n = 3$).

(Fig. S18 in Supporting information) [36]. Flow cytometry enabled rapidly collecting the multifaceted characteristics information from a large cell population and sort out specific cells. A single cell suspension was prepared using HT-29 cells, and the cell concentration was adjusted to 2×10^6/mL. HT-29 cells were divided into test group and control group, cells of test group treated with 1, 2, 5 μmol/L SNI and 40, 80, 200 μg/mL SNI@ZIF-8 were incubated for 40 min and were washed 3 times by PBS buffer, and the intensity of emission and the amount of stained cells were recorded by flow cytometry (Fig. 3a) [37]. In the presence of SNI and SNI@ZIF-8, the geometric mean of the fluorescence intensity showed considerably elevation. Whether SNI@ZIF-8 could be applied to image cell membrane region was confirmed by co-stain HT-29 cells dealing with a dye DIO (3,3′-dioctadecyloxacarbocyanine perchlorate). The cells were prepared by incubation with DIO (1 μmol/L, green channel) and SNI (0.5, 1 and 2 μmol/L, red channel) for 5 min in PBS buffer [38]. Cell confocal imaging results were consistent with flow cytometry results. As shown in Fig. 3b and Fig. S20 (Supporting information), the curve fitting of the two channels was conducted and the distribution of fluorescence intensity was basically similar. Meanwhile, with the increase of SNI concentration, the mean fluorescence intensity of cells also increased gradually. Note that the green fluorescence images matched well with the red fluorescence images in HT-29 cells, respectively. The membrane localization ability of SNI@ZIF-8 was evaluated, co-localization staining of HT-29 cells was performed for 5 min using DIO (1 μmol/L, green channel) and SNI@ZIF-8 (20, 40 and 60 μg/mL, red channel). As shown in Fig. 3b and Fig. S21 (Supporting information), the fluorescence distribution of red and green channels was basically the same, and the cell fluorescence intensity increased with the increase of SNI@ZIF-8 concentration (Fig. 3c), which had a good co-localization effect with commercially fluorescent dye DIO. SNI@ZIF-8 showed local accumulation of the generated signal and specially located in the plasma membrane distribution. Exploring the cell endocytosis and the targeting of host-guest system is the one should be focus of attention. The cells were treated with the same concentration of ZIF-8 and SNI@ZIF-8 respectively, and the accumulation of zinc ions in the cells was detected to characterize the enhancement of the targeting effect of SNI on the host-guest system. And the inductively coupled plasma-mass spectrometry (ICP) result further indicated that SNI@ZIF-8 is more easily ingested by cells, which further verifies the targeting property of SNI@ZIF-8 (Fig. 3c) [39,40]. Small molecule inhibition of tyrosine kinases was designed by inhibiting intracellular regions of adenosine triphosphate (ATP) binding sites [41]. Other types of inhibitors competed with molecular skeleton binding sites to inhibit HT-29 cell recognition *via* SNI@ZIF-8. The fluorescence intensity decreased after the addition of gefitinib and sorafenib (VEGFR inhibitor), which was not significantly different from that of axitinib and erlotinib (epidermal growth factor receptor inhibitor) (Fig. 3d). As shown experimentally, SNI@ZIF-8 achieved targeted enrichment and stable cell membrane imaging in overexpressing RTKs cells. Moreover, SNI with a Sunitinib skeleton demonstrated similar effects to RTKs inhibitors in inhibiting downstream VEGF-A protein expression, and SNI@ZIF-8, which contained zinc ions, exhibited the ability to affect the intracellular caspase-1 signaling pathway (Figs. S23, S24 and S30 in Supporting information) [42-45]. Consequently, the host-guest system SNI@ZIF-8 had excellent biocompatibility and imaging capabilities within HT-29 cells, supporting its participation in cellular immunotherapy as an integrated imaging and therapeutic host and client system.

Hemolysis test was used to evaluate the possibility of application of host-guest system *in vivo*. As shown in Fig. 3e, ZIF-8 and SNI@ZIF-8 could not cause a lot of destruction of red blood cells, which proved that host-guest system SNI@ZIF-8 is suitable for application in life system. As shown in Fig. 4a, a xenografted mouse model was used to further assess its capability for the real-time visualization of RTKs [46,47]. Animal experiments were approved by the Biological and Medical Ethics Committee of Dalian University of Technology. The 100 μL HT-29 cell suspensions with cell density of 1×10^7/mL were subcutaneously injected to 5–8 weeks old BALB/c-nu nude mice with equal volume to establish xenograft model. All of the mice received injection of the cancer cells in the outside of armpits, after 10–15 days the tumors were allowed to grow to 400–800 mm^3 established the animal model of HT-29 transplanted. The HT-29 transplanted mice received intravenous injections the probe SNI (100 μmol/L, 100 μL) and SNI@ZIF-8 (4 mg/mL, 100 μL) into the cancer and fluorescence signal were monitored for 0.5, 2, 4, 6, 12 and 24 h time interval [48]. Both probes exhibited steadily enhanced fluorescence signals over time for 6 h, and the fluorescence signals were not obvious after 24 h. Moreover, the nanosizing of SNI enabled the nanoprobe to accumulate at the tumor site for a longer time and release

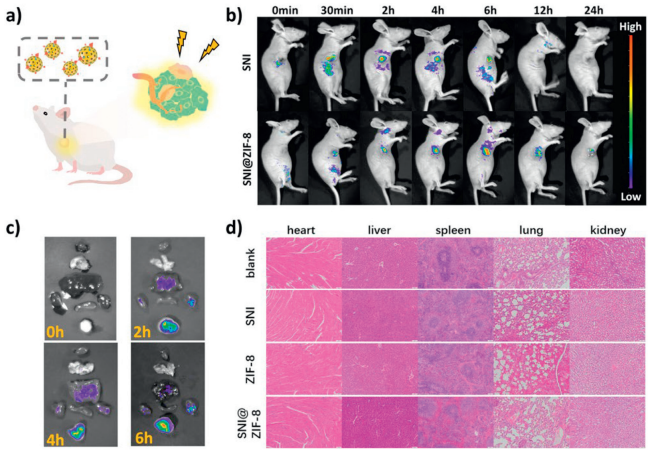

Fig. 4. (a) Imaging diagram of SNI@ZIF-8 at the tumor site. (b) *In vivo* fluorescence imaging of the HT-29 tumor mouse model at different time interval. The fluorescence signal was collected at 570 nm. (c) *Ex vivo* image of the heart, liver, spleen, lung, kidney and tumor fluorescence of HT-29 tumor mouse model with the probe SNI@ZIF-8 (4 mg/mL, 100 μL) at different time interval (0, 2, 4 and 6 h). (d) H&E staining maps of major organs tissues of mice treated with SNI, ZIF-8 and SNI@ZIF-8. Scale bar: 200 μm.

the small molecule probe SNI, making it obtain a longer fluorescence signal in mice than SNI (Fig. 4b). *Ex vivo* fluorescence images of tissue which is dissected from xenografted mouse model, show that tumor still displayed strong fluorescence signal and no fluorescence signal was obtained from heart, spleen and lung (Fig. 4c). Hematoxylin-eosin (H&E) staining showed no significant histopathological damage in major organs of mice injected with SNI and SNI@ZIF-8 (Fig. 4d) [49]. These results indicated that host-guest system SNI@ZIF-8 selectively accumulated tumor tissues and low background fluorescence signal was obtained from other normal organs. Hence, SNI@ZIF-8 can be employed to identify and visualize in biosystems for clearly located tumor, the SNI@ZIF-8 has the ability for real-time imaging tumor tissues [17].

In summary, the host-guest system SNI@ZIF-8 has been proposed and constructed as a fluorescent probe that can interact with RTKs on the cell membrane. SNI@ZIF-8 exhibits high selectivity and photostability to VEGFR-2 in simulated physiological media with excellent fluorescence emission response. SNI@ZIF-8 is able to accurately locate the VEGFR-2 overexpressed cancer cells and accumulate in these cells, enabling fluorescence imaging for effectively distinguishing tumor tissues with low background interference in tumor-bearing mice. Prospectively, the host-guest system SNI@ZIF-8 provides a reliable means for recognizing RTKs in early diagnosis, monitoring and prognosis of cancer.

Declaration of competing interest

The authors declare that they have no known competing financial interests or personal relationships that could have appeared to influence the work reported in this paper.

CRediT authorship contribution statement

Meng Gao: Writing – original draft, Data curation. **Jiqiu Yin:** Methodology, Data curation. **XianChao Jia:** Investigation. **Ye Gao:** Investigation. **Yang Jiao:** Writing – review & editing, Supervision, Conceptualization.

Acknowledgment

This work was supported by the National Natural Science Foundation of China (Nos. 22338005, 21977015).

Supplementary materials

Supplementary material associated with this article can be found, in the online version, at doi:10.1016/j.cclet.2024.110297.

References

[1] C. Leslie, K. Hanna, G. Massimo, et al., Nat. Rev. Immunol. 23 (2023) 787–806.
[2] D. Deborah, H. Justus, E. Shelton, et al., Nat. Rev. Clin. Oncol. 20 (2023) 755–779.
[3] R. Daly, A. Scott, O. Klein, et al., Mol. Cancer 21 (2022) 189.
[4] H. Singh, Y. Li, L. Spurr, et al., Clin. Cancer Res. 27 (2021) 1695–1705.
[5] X. Ma, M. Mao, J. He, et al., Chem. Soc. Rev. 52 (2023) 6447–6496.
[6] K. Wang, C. Liu, H. Zhu, et al., Coordin. Chem. Rev. 477 (2023) 214946.
[7] J. Tan, H. Li, L. Zhang, et al., Nat. Commun. 13 (2022) 594.
[8] J. Liu, J. Fraire, S. Smedt, R. Xiong, K. Braeckmans, Small 16 (2020) 2000146.
[9] X. Wu, R. Wang, N. Kwon, et al., Chem. Soc. Rev. 51 (2022) 450–463.
[10] Z. Wang, J. Li, J. Chen, et al., Chin. Chem. Lett. 34 (2023) 108507.
[11] H. Zhu, K. Ma, R. Ruan, et al., Chin. Chem. Lett. 35 (2024) 108536.
[12] W. Liu, Q. Qiao, J. Zheng, et al., Biosens. Bioelectron. 176 (2021) 112886.
[13] Z. Li, P. Liang, T. Ren, et al., Angew. Chem. Int. Ed. 62 (2023) e202305742.
[14] P. Liu, F. Fang, H. Wang, et al., Angew. Chem. Int. Ed. 62 (2023) e202218706.
[15] Y. Wang, H. Wu, W. Hu, et al., Adv. Mater. 34 (2022) 2105405.
[16] R. Kankala, Adv. Drug Deliv. Rev. 186 (2022) 114270.
[17] H. Wang, L.Zhang P.Liang, Chin. Chem. Lett. 34 (2023) 108129.
[18] I. Sterin, J. Hadynski, A. Tverdokhlebova, et al., Adv. Mater. 36 (2024) 2308640.
[19] E. Linnane, S. Haddad, F. Melle, et al., Chem. Soc. Rev. 51 (2022) 6065–6086.
[20] C. Zhou, J. Chen, B. Zheng, et al., ACS Appl. Mater. Interfaces 15 (2023) 44731–44741.
[21] C. Liu, L. Guo, Y. Wang, et al., Coordin. Chem. Rev. 494 (2023) 215332.
[22] M. Kahlson, S. Dixon, Science 375 (2022) 6586.
[23] H. Lei, G. Hou, M. Chen, et al., Nano Today 53 (2023) 102033.
[24] M. Yan, S. Wu, Y. Wang, et al., Adv. Mater. 36 (2024) 2304249.
[25] N. Ebrahimi, E. Fardi, H. Ghaderi, et al., Cell. Mol. Life Sci. 80 (2023) 104.
[26] J. Li, Q. Qiao, Y. Ruan, et al., Chin. Chem. Lett. 34 (2023) 108266.
[27] N. Singer, P. Sánchez-Murcia, M. Ernst, et al., Angew. Chem. Int. Ed. 61 (2022) e202205198.
[28] J. Jin, Y. Zhang, J. Zhang, et al., Drug Resist. Updat. 67 (2023) 100929.
[29] M. McTigue, B. Murray, J. Chen, et al., Proc. Natl. Acad. Sci. U. S. A. 109 (2012) 18281–18289.
[30] Y. More, S. Mollick, S. Saurabh, et al., Small 20 (2024) 2302014.
[31] L. Kong, S. Lv, Z. Qiao, et al., Biosens. Bioelectron. 207 (2022) 114188.
[32] J. Zhong, J. Zhou, M. Xiao, et al., Chin. Chem. Lett. 33 (2022) 973–978.
[33] H. Yuan, N. Li, W. Fan, et al., Adv. Sci. 9 (2022) 2104374.
[34] B. Shen, C. Ma, Y. Ji, et al., ACS Appl. Mater. Interfaces 13 (2021) 8718–8726.
[35] B. Morozov, F. Gargiulo, S. Ghule, et al., J. Am. Chem. Soc. 146 (2024) 7105–7115.
[36] J. Xing, Q. Gong, R. Zou, et al., Chin. Chem. Lett. 34 (2023) 107786.
[37] D. Berndt, D. Glaap, T. Jennings, et al., Angew. Chem. Int. Ed. (2024) e202402616.
[38] H. Zhao, N. Li, C. Ma, et al., Chin. Chem. Lett. 34 (2023) 107699.
[39] S. Jeon, C. Castillo, V. Nava, et al., Small 20 (2024) 2304588.
[40] H. Cheng, C. Wang, Z. Lyu, et al., J. Am. Chem. Soc. 145 (2023) 1216–1226.
[41] A. Basolo, A. Matrone, R. Elisei, et al., Semin. Cancer Biol. 79 (2022) 197–202.
[42] X. Qi, M. Yang, L. Ma, et al., J. Immunother. Cancer 8 (2020) e001038.
[43] L. Tu, C. Li, X. Xiong, et al., Angew. Chem. Int. Ed. (62) (2023) e202301560.
[44] C. Li, L. Tu, J. Yang, et al., Chem. Sci. 14 (2023) 2901.
[45] L. Xu, M. Peng, T. Gao, et al., Adv. Sci. 11 (2024) 2306203.
[46] R. Chen, W. Li, R. Li, et al., Chin. Chem. Lett. 34 (2023) 107845.
[47] Y. Xu, C. Li, J. An, et al., Sci. China Chem. 66 (2023) 155.
[48] A. Yadav, Z. Zhao, Y. Weng, et al., J. Am. Chem. Soc. 145 (2023) 1460–1469.
[49] H. Yuan, Z. Han, Y. Chen, et al., Angew. Chem. Int. Ed. 60 (2021) 8174–8181.